AIAA JOURNAL
Vol. 33, No. 9, September 1995

Structural/Control System Optimization with Variable Actuator Masses

Ik Min Jin*
Korea Aerospace Research Institute, Taejon, Republic of Korea
and
Abdon E. Sepulveda†
University of California, Los Angeles, Los Angeles, California 90095

A method is presented to integrate the design space for structural/control system optimization problems in the case of linear state feedback control. Nonstructural lumped masses and control system design variables as well as structural sizing variables are all treated equally as independent design variables in the optimization process. Structural and control design variable linking schemes are used in order to avoid a prohibitively large increase in the total number of independent design variables. When actuator masses are treated as nonstructural lumped mass design variables, special consideration is given to the relation between the transient peak responses and the required actuator masses that is formulated as a behavior constraint form. A method to prevent instability of uncontrolled higher modes by modifying the feedback gain matrix without information about higher modes is also presented. The original nonlinear mathematical programming problem based on a finite element formulation and linear state feedback is replaced by a sequence of explicit approximate problems exploiting various approximation concepts such as design variable linkings, temporary constraint deletion, and first-order Taylor series expansion of nonlinear behavior constraints in terms of intermediate design variables. Examples which involve a variety of dynamic behavior constraints (including constraints on closed-loop eigenvalues, peak transient displacements, peak actuator forces, and relations between the peak responses and the actuator masses) are effectively solved by using the method presented.

Introduction

IN the context of structural/control system optimization problems it is usually assumed that the mass of the control actuators are assigned to be fixed during the entire design process.[1–7] In Refs. 8–10, the design objectives to be minimized include the structural masses and the equivalent masses for the controller which are assumed to be a simple analytical function of the control effort or the peak actuator torque. Reference 9 treats structural sizing variables and damping factors as design variables, and actuator masses are approximated according to the assumed relation between the control effort and the actuator mass. In Ref. 10, it is assumed that actuator masses are fixed during one cycle of optimization, and they are updated after finding transient peak control torque values of the new design according to the functional or empirical relations between the maximum peak control torques and the required actuator mass. But in these references, actuator masses are not considered as independent design variables in the optimization process.

The main purpose of this study is to include the actuator masses in a set of independent design variables while satisfying a certain relation between the transient peak responses and the required actuator masses (actuator mass constraints). This is done by expressing the peak control forces in a closed-form solution, which can be treated as behavior constraints in the optimization cycle, and by exploiting the control design variable linking schemes introduced in Refs. 1 and 2. A simple method to resolve the spillover effects by modifying the feedback gain matrix without information about higher modes is also presented.

Problem Statements

The simultaneous structural/control optimization problem is formulated as a general nonlinear inequality constrained mathematical programming problem as follows:

$$\begin{aligned} &\text{find } \boldsymbol{Y} \text{ to minimize } F(\boldsymbol{Y}) \\ &\text{subject to } G_j(Y) \le 0, \qquad j = 1, \ldots NCON \\ &\text{with bounds } Y_i^L \le Y_i \le Y_i^U, \qquad i = 1, \ldots, NDV \end{aligned} \tag{1}$$

where NDV is the total number of design variables, $\boldsymbol{Y} = [Y_1, Y_2, \ldots, Y_{\text{NDV}}]^T$ is an $NDV \times 1$ design variable vector, F is a scalar objective function, G_j is the jth behavior constraint, $NCON$ is total number of behavior constraints, and Y_i^L and Y_i^U are side constraints on the ith design variable, respectively.

Nonstructural lumped mass variables representing variable actuator masses are included independently in the design variable vector $\boldsymbol{Y}$ in addition to the structural sizing variables and control design variables. The mass of the actuators is included in the mass matrix of the system and, therefore, their influence in the system modes is captured. The total mass of the system (structural mass plus nonstructural mass) has been chosen as the objective function with constraints on 1) dynamic stability (real parts of closed-loop eigenvalues), 2) damped frequencies (imaginary parts of closed-loop eigenvalues), 3) peak transient responses, 4) peak transient control forces, and 5) required actuator masses, included in this study.

Structural/Control System Description

The second-order equations of motion based on the finite element method are

$$[M]\{\ddot{q}\} + [C]\{\dot{q}\} + [K]\{q\} = [b]\{u\} + [e]\{f\} \tag{2}$$

where $\{q\}$ is an $N \times 1$ vector of nodal degrees of freedom (DOF); $\{\dot{q}\}$ and $\{\ddot{q}\}$ are first and second time derivatives of $\{q\}$; $[M]$, $[K]$, and $[C]$ are $N \times N$ mass, stiffness, and damping matrices, respectively; $\{u\}$ is an $M \times 1$ actuator force vector, M is the number of actuators; $\{f\}$ is an $L \times 1$ vector of external disturbances; L is the number of external disturbances making up a single load condition; and $[b]$ and $[e]$ are $N \times M$ and $N \times L$ coefficient matrices consisting of the directional cosines which relate actuator and disturbance forces to the nodal DOFs, respectively.

Presented as Paper 93-1473 at the AIAA/ASME/ASCE/AHS/ASC 34th Structures, Structural Dynamics, and Materials Conference, La Jolla, CA, April 19–22, 1993; received May 6, 1994; revision received Jan. 4, 1995; accepted for publication Jan. 5, 1995.

*Senior Researcher. Member AIAA.
†Assistant Professor, Department of Mechanical, Aerospace and Nuclear Engineering. Member AIAA.

It is assumed that the preassigned damping inherent to the structure can be represented by a proportional damping matrix, which is a linear combination of the system mass and stiffness matrices, i.e.,

$$[C] = c_M[M] + c_K[K] \tag{3}$$

Equation (2) can be transformed into the first-order state-space equation as follows:

$$\{\dot{x}\} = [A_0]\{x\} + [B]\{u\} + [E]\{f\} \tag{4}$$

where

$$\{x\}^T = \lfloor \{q\}^T \quad \{\dot{q}\}^T \rfloor$$

$$[A_0] = \begin{bmatrix} [0] & [I] \\ -[M]^{-1}[K] & -[M]^{-1}[C] \end{bmatrix}$$

$$[B] = \begin{bmatrix} [0] \\ -[M]^{-1}[b] \end{bmatrix}$$

The control input vector $\{u\}$ is to be determined under the assumption that all of the states (components of $\{x\}$) are available, that is,

$$\{u\} = -[H]\{x\} = -[H_p]\{q\} - [H_v]\{\dot{q}\} \tag{5}$$

where $[H]$ is the $M \times 2N$ feedback gain matrix, and $[H_p]$ and $[H_v]$ are the $M \times N$ position and velocity parts of $[H]$, respectively. The closed-loop state equation becomes

$$\{\dot{x}\} = [A]\{x\} + [E]\{f\} \tag{6}$$

where the closed-loop system matrix $[A]$ is

$$[A] = [A_0] - [B][H]$$

The feedback gain matrix $[H]$ is expressed as a linear combination of the basis matrices as follows[2]:

$$[H] = \sum_{i=1}^{r} \alpha_i [H^0]^{(i)} \tag{7}$$

where $[H^0]^{(i)}$ is the ith $M \times 2N$ basis matrix calculated by the ith 2×2 Riccati equation, r the number of modes considered, and α_i the corresponding coefficient which is used as the independent design variable during the optimization cycle (see Ref. 2).

Actuator Mass Constraints

The actuators, located at specified structural nodes, can be sized so that they produce control forces or torques required to suppress the vibration. In Refs. 8–10, actuator masses are assumed to have a simple functional relationship with the control effort or the peak actuator torque. In this study a relationship between the peak control forces and the required actuator masses is assumed as follows:

$$m_A \geq c_1 |u(t)|^{c_2}, \qquad 0 \leq t \leq t_{\max} \tag{8}$$

where m_A is the mass of the actuator, $t_{\max}$ is the time interval of interest, and c_1 and c_2 are constants relating the peak control forces and required actuator masses.

Assuming that the external disturbance $\{f(t)\}$ can be expressed in terms of a truncated Fourier series and polynomials over a specified period of time, Eq. (6) can be integrated with respect to time in closed form and form Eq. (5) transient control forces can also be calculated in closed form (see Ref. 1).

Time-dependent actuator mass constraints in Eq. (8) can now be replaced with a finite number of peak time constraints by first finding the corresponding peak times of the control forces using the adaptive one dimensional search method described in Ref. 11, namely,

$$m_A \geq c_1 |u(t_j^*)|^{c_2}, \qquad j = 1, \ldots, NPEAK \tag{9}$$

where t_j^* is the jth peak time of control forces or torques and $NPEAK$ is the number of control force peak times. Equation (9) can be normalized such that

$$G = \frac{c_1 |u(t_j^*)|^{c_2}}{m_A} - 1 \leq 0, \qquad j = 1, \ldots, NPEAK \tag{10}$$

The sensitivity of the actuator mass constraint with respect to an arbitrary design variable α is obtained by differentiating Eq. (10),

$$\begin{aligned} \frac{\partial G}{\partial \alpha} &= c_1 \frac{\partial}{\partial \alpha}\left(\frac{|u(t_j^*)|^{c_2}}{m_A}\right) \\ &= c_1 \left[\frac{c_2}{m_A} \{u(t_j^*)\}^{c_2 - 1} \frac{\partial u(t_j^*)}{\partial \alpha} \right. \\ &\quad \left. + \{u(t_j^*)\}^{c_2} \frac{\partial}{\partial \alpha}\left(\frac{1}{m_A}\right)\right], \qquad u(t_j^*) \geq 0 \\ &= c_1 \left[-\frac{c_2}{m_A} \{-u(t_j^*)\}^{c_2 - 1} \frac{\partial u(t_j^*)}{\partial \alpha} \right. \\ &\quad \left. + \{-u(t_j^*)\}^{c_2} \frac{\partial}{\partial \alpha}\left(\frac{1}{m_A}\right)\right], \qquad u(t_j^*) < 0 \end{aligned} \tag{11}$$

In Eq. (11), $\partial u(t_j^*)/\partial \alpha$ is the sensitivity of the peak control forces, and $\partial/\partial\alpha(1/m_A)$ is nonzero only when α is the corresponding actuator mass variable.

Spillover Effect

In this section, the existence of spillover effect (see Ref. 12) of the formulation used in this study is investigated. Consider Eq. (2) without external disturbance force $\{f\}$ and Eq. (5) again:

$$[M]\{\ddot{q}\} + [C]\{\dot{q}\} + [K]\{q\} = [b]\{u\} \tag{12}$$

$$\{u\} = -[H_p]\{q\} - [H_v]\{\dot{q}\} \tag{13}$$

The nodal degree of freedom vector $\{q\}$ can be written without any truncation as follows [compare with Eq. (16) of Ref. 1]:

$$\{q\} = [V_C]\{z_C\} + [V_U]\{z_U\} \tag{14}$$

where $\{z_C\}$ is the $r \times 1$ controlled normal coordinate vector, $[V_C]$ is the $N \times r$ eigenmatrix consisting of the controlled r normal eigenvectors, $\{z_U\}$ is the $(N - r) \times 1$ uncontrolled normal coordinate vector, and $[V_U]$ is the $N \times (N - r)$ eigenmatrix corresponding to uncontrolled modes $\{z_U\}$.

Eigenmatrices $[V_C]$ and $[V_U]$ in Eq. (14) are normalized such that

$$\begin{aligned} [V_C]^T[M][V_C] &= [I] \\ [V_U]^T[M][V_U] &= [I] \\ [V_C]^T[M][V_U] &= [0] \end{aligned} \tag{15}$$

and

$$\begin{aligned} [V_C]^T[K][V_C] &= [\Lambda_C] \\ [V_C]^T[C][V_C] &= [C_C] \\ [V_U]^T[K][V_U] &= [\Lambda_U] \\ [V_U]^T[C][V_U] &= [C_U] \end{aligned} \tag{16}$$

Substituting Eq. (14) into Eq. (12), premultiplying by $[V_C]^T$ and $[V_U]^T$, and using the orthogonality properties results in the equations for controlled and uncontrolled modes, i.e.,

$$\{\ddot{z}_C\} + [C_C]\{\dot{z}_C\} + [\Lambda_C]\{z_C\} = [V_C]^T[b]\{u\} \tag{17}$$

$$\{\ddot{z}_U\} + [C_U]\{\dot{z}_U\} + [\Lambda_U]\{z_U\} = [V_U]^T[b]\{u\} \tag{18}$$

On the right-hand side of Eq. (18), $[V_U]^T[b] \neq [0]$, which means there exists control spillover.

Substituting Eq. (14) into Eq. (13) leads to

$$\begin{aligned} \{u\} = &-([H_p][V_C]\{z_C\} + [H_v][V_C]\{\dot{z}_C\}) \\ &- ([H_p][V_U]\{z_U\} + [H_v][V_U]\{\dot{z}_U\}) \end{aligned} \tag{19}$$

On the right-hand side of Eq. (19), those matrices in front of the uncontrolled modes are not zero (i.e., $[H_p][V_U] \neq [0]$, $[H_v][V_U] \neq [0]$) which can be interpreted as observation spillover.

As can be seen from Eqs.(18) and (19), there exist both control and observation spillover. According to Ref. 12, the closed-loop system has potential instability when the system has both observation and control spillover, and it is more important to eliminate observation spillover in order to prevent instability. Therefore, the desired control input $\{u^*\}$ should contain only controlled modes $\{z_C\}$, namely,

$$\{u^*\} = -[H_p][V_C]\{z_C\} - [H_v][V_C]\{\dot{z}_C\} \tag{20}$$

Premultiplying $[V_C]^T[M]$ to Eq. (14) and using relations in Eq. (15) results in

$$\{z_C\} = [V_C]^T[M]\{q\} \tag{21}$$

Substituting Eq. (21) into Eq. (20) gives

$$\begin{aligned}\{u^*\} &= -[H_p][V_C][V_C]^T[M]\{q\} - [H_v][V_C][V_C]^T[M]\{\dot{q}\} \\ &= -[H_p^*][M]\{q\} - [H_v^*]\{\dot{q}\}\end{aligned} \tag{22}$$

where

$$[H_p^*] = [H_p][V_C][V_C]^T[M] \tag{23}$$

and

$$[H_v^*] = [H_v][V_C][V_C]^T[M] \tag{24}$$

In summary, destabilization of uncontrolled higher modes can be prevented by using the truncated feedback gain matrices just shown since these matrices are orthogonal to the uncontrolled higher modes $[V_U]$ and will eliminate observation spillover.

Optimization

Various approximation concepts, such as structural and control design variable linking, temporary constraint deletion, and intermediate design variables,[13,14] are used to replace the original design optimization problem by a series of explicit approximate problems. Linear, reciprocal, or hybrid approximations (see Ref. 15) can be generated with respect to either direct or intermediate design variables, even though the approximate design optimization problems are always solved in an integrated design space that spans the independent structural sizing variables, actuator mass variables, and the participation coefficients of the linked control gains. Each approximate optimization problem has its own lower and upper bounds on the design variables. These bounds are determined by the move limits to protect the quality of the approximations or by the original side constraints [see Eq. (1)], whichever is most restrictive. For frame elements it is known that the section properties A, Iy, Iz, and J are a good choice for intermediate design variables. This follows from the fact that the elements of the stiffness and the mass matrices are linear functions of these section properties. Control design variables α_i are used directly in the generation of the approximate problem because the system matrices are linear functions of the gains.

With the information acquired from the analysis and sensitivity analysis phase each approximate optimization problem can be formulated as follows:

$$\begin{aligned}&\text{find } \boldsymbol{Y} \text{ to minimize } \tilde{F}[\boldsymbol{X}(\boldsymbol{Y})] \\ &\text{subject to } \tilde{G}_j[\boldsymbol{X}(\boldsymbol{Y})] \leq 0, \qquad j \in Q_R \\ &\text{with bounds } \tilde{Y}_i^L \leq Y_i \leq \tilde{Y}_i^U, \qquad i = 1, \ldots, NDV\end{aligned} \tag{25}$$

where NDV is the total number of design variables, $\boldsymbol{Y}$ is a vector of design variables ($NDV \times 1$), $\boldsymbol{X}(\boldsymbol{Y})$ is a vector of intermediate design variables, $\tilde{F}(\cdot)$ is an approximate objective function, $\tilde{G}_j(\cdot)$ is the jth approximate constraint, $\tilde{Y}_i^L$ and $\tilde{Y}_i^U$ are lower and upper bounds for the ith design variable (during solution of the current approximate optimization problem), and Q_R is the retained set of constraints for the current approximate problem. For all of the numerical examples presented in this paper, the following approximation options are employed. Linear approximation of $\tilde{F}(\cdot)$ is used with respect to intermediate structural design variables (A, Iy, Iz, J) which is exact when the mass is minimized. When generating the approximate constraint functions $\tilde{G}_j(\cdot)$ linear approximation is chosen with respect to control design variables and actuator mass variables whereas the hybrid approximation is used with respect to structural intermediate design variables.

Numerical Results

The control augmented structural optimization solution method described previously has been implemented on the IBM ES/9000 Model 900 supercomputer at University of California, Los Angeles. CONMIN[16] is used as the optimizer, and it is conservatively assumed that the passive damping is zero [$c_M = c_K = 0$, see Eq. (3)]. The convergence criterion used in these examples is that the relative change in the objective function values between two sets of consecutive design iterations should be less than 0.1%.

The example problem chosen is an antenna structure drawn from Ref. 2 consisting of eight aluminium beams ($E = 7.3 \times 10^6$ N/cm^2, $p = 2.77 \times 10^{-3}$ kg/cm^3, $v = 0.325$) that have thin-walled hollow box beam cross sections (see Fig. 1). This structure is constrained to move vertically (Y direction) only, so each nodal point has 3 degrees of freedom (translation, bending, and torsion) resulting in the total 18 degrees of freedom ($N = 18$). Four translational actuators (actuator 1–4) with initial weight of 4 kg each are attached to nodes 3, 5, 6, and 7 (with side constraints 0.1 kg $\leq m_A \leq$ 100 kg). These actuators are oriented so that the force they generate acts in the vertical direction (degrees of freedom 4, 10, 13, and 16). Two ramp type transient loads are applied to the node 3 at the same time. One is a vertical force $[f_1(t)]$ and the other is a torsional moment $[f_2(t)]$ with respect to finite elements 1 and 2 which gives antisymmetric excitation. These loads are given as follows:

$$f_1(t) = 333.3t \text{ N}, \qquad f_2(t) = 10 \times f_1(t) \text{ N} \cdot \text{cm}$$

for $0 \leq t \leq 0.3$ s, and $f_1(t) = f_2(t) = 0$ for $t > 0.3$ s (see Fig. 1). Transient responses are considered for the time interval $0 \leq t \leq 2$ s, and 20 out of 36 complex modes are used to calculate the peak response values.

Flange and web thicknesses are constrained to be the same, so there are three structural design variables for each finite element (B, H, and $T = T2 = T3$). Structural linking is used to make the structure remain symmetric with respect to the XY plane, and also masses of the actuator number 2 and 4 are linked to be the same which results in the 15 independent structural design variables and 3 independent lumped mass variables. The initial structure is uniform ($B = H = 20.0$ cm, $T = 0.5$ cm), and the side constraints are 10.0 cm $\leq B, H \leq$ 25.0 cm, and 0.1 cm $\leq T \leq$ 1.0 cm.

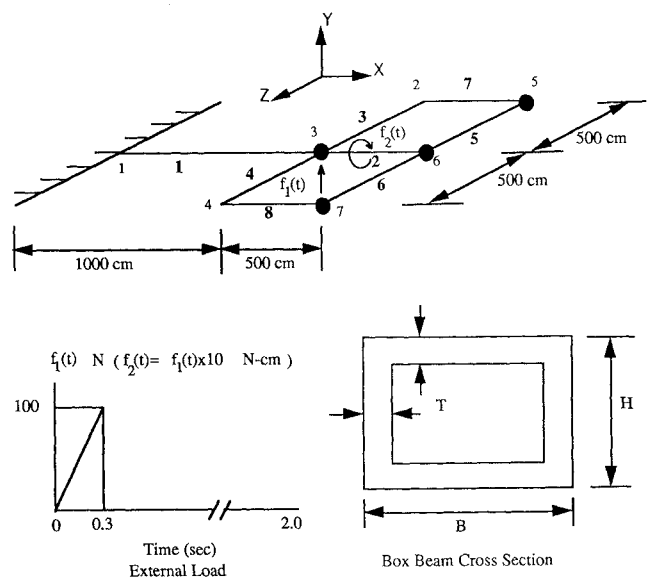

Fig. 1 Antenna structure.

Move limits of 30% are used for all kinds of design variables. The design objective is to minimize the total mass of the system including both the structural masses and the nonstructural actuator masses. Behavior constraints are imposed on (see Refs. 1, 2, and 17) 1) the real part of all the retained complex modes ($\sigma_i \leq -0.5$), 2) the fourth and fifth damped frequencies ($\omega_{d4} \leq 8.0$ Hz, $\omega_{d5} \leq 9.25$ Hz), 3) the peak displacement of nodes 2, 4, 5, and 7 [$q_i(t) \leq 1.0$ cm, $i = 1, 7, 10$, and 16], 4) the peak actuator force [$u_j(t) \leq 8.5$ N, $j = 1, 2, 3$, and 4], and 5) actuator mass constraints which will be explained in detail later on. For each approximate problem, all of the eigenvalue constraints are retained, but the transient constraints are retained in Q_R only when the response ratio (response value divided by the allowable response value) is greater than 0.3.

Initial feedback gains are computed by solving 10 sets of 2×2 Riccati equations ($r = 10$) with the control weighting coefficients $\gamma_i = 1/400$ and the state weighting matrices $[Q_i] = \text{diag}(\omega_i^2, 1)$, $i = 1, \ldots, r$ (see Ref. 1). All 10 participation coefficients α_i in Eq. (7) are used as independent control system design variables.

As a reference solution, the coefficients in Eq. (9) are chosen such that $c_1 = 4\,\text{kg}/8.5\,\text{N} = 0.0047\ \text{s}^2/\text{cm}$ and $c_2 = 1$, which is similar to case 10 of Ref. 2 where actuator masses are fixed to be 4 kg and the peak actuator forces are constrained to be less than 8.5 N. Iteration histories, final cross-sectional dimensions, and final actuator masses of the reference run are compared with those of case 10 of Ref. 2 (see Tables 1 and 2). As expected, these two runs are quite similar with each other in the iteration histories and final designs except the actuator masses. The major change on the actuator masses occurs for actuator number 1 of which optimal mass is 2.7 kg, whereas the major changes on the cross-sectional dimensions are on B of elements 3, 4, 7, and 8, but the final optimal weight is similar to (in fact, slightly smaller than) that of Ref. 2 (i.e., compare 170.92 and 170.17 kg), which is expected since the parameters c_1 and c_2 are chosen to match the conditions of case 10 in Ref. 2. This result can be interpreted as that the optimization process puts smaller mass for actuator number 1 since the peak actuator force of actuator number 1 is smaller than those of the other actuators, and redistributes weight on elements 3, 4, 7, and 8.

The main importance of using Eq. (8) to relate the actuator masses and the maximum output forces is that it enables more flexibility in the design space, since it allows the designer to choose the actuator (mass and output force) after the optimization process and not before, as in the case of fixed actuator masses.

The influence of the coefficient c_1 is investigated with the exponent in Eq. (9) set to be unity ($c_2 = 1$). The value of c_1 is varied from 0.001 s^2/cm to 0.01 s^2/cm. The final optimal masses are given with respect to different c_1 values in Table 3 and graphically in Fig. 2. As representative cases, iteration histories of $c_1 = 0.001$, 0.0047, and 0.01 s^2/cm are shown in Fig. 3, and those final structural designs and final actuator masses are given in Table 4. From Fig. 2 it is seen that the optimal mass is almost linear with respect to c_1 (for fixed c_2). This linear relation is quite reasonable since c_1 determines the maximum actuator mass for a given maximum output

Table 1 Iteration histories fixed and variable actuator masses

Analysis number	Fixed actuator masses, case 10 of Ref. 2	Variable actuator masses, $c_1 = 0.0047\ \text{s}^2/\text{cm}$, $c_2 = 1$
1	502.14	502.14
2	469.10	476.98
3	350.45	354.56
4	268.09	270.96
5	215.51	213.92
6	181.84	184.34
7	173.50	173.01
8	171.19	171.14
9	171.02	170.62
10	170.96	170.34
11	170.92	170.23
12		170.17

Table 3 Coefficient c_1 vs final masses, $c_2 = 1$

c_1, s^2/cm	Final mass, kg
0.001	159.81
0.002	164.98
0.003	166.44
0.004	168.59
0.0047	170.17
0.005	170.67
0.006	173.40
0.007	175.38
0.008	176.98
0.009	179.10
0.010	182.67

Table 2 Final cross-sectional dimensions and actuator masses fixed and variable actuator masses

Design variables	Element/actuator number		Fixed actuator masses, case 10 of Ref. 2	Variable actuator masses, $c_1 = 0.0047\ \text{s}^2/\text{cm}$, $c_2 = 1$
Final cross-sectional dimensions, cm	1	B	25.00[b]	25.00[b]
		H	25.00[b]	25.00[b]
		T	0.1000[a]	0.1000[a]
	2	B	25.00[b]	25.00[b]
		H	25.00[b]	25.00[b]
		T	0.1058	0.1000[a]
	3,4	B	19.96	18.26
		H	25.00[b]	25.00[b]
		T	0.1000[a]	0.1000[a]
	5,6	B	25.00[b]	25.00[b]
		H	25.00[b]	25.00[b]
		T	0.2296	0.2330
	7,8	B	20.96	22.80
		H	25.00[b]	25.00[b]
		T	0.1000[a]	0.1000[a]
Final actuator masses, kg	1		4.0[c]	2.700
	2 and 4		4.0[c]	4.006
	3		4.0[c]	3.920

[a]Lower bound values. [b]Upper bound values. [c]Fixed masses.

Table 4 Final cross-sectional dimensions and actuator masses with different c_1 ($c_2 = 1$)

Design variables	Element/actuator number		$c_1 = 0.001$ s^2/cm	$c_1 = 0.01$ s^2/cm
Final cross-sectional dimensions, cm	1	B	25.00[b]	25.00[b]
		H	25.00[b]	25.00[b]
		T	0.1110	0.1000[a]
	2	B	25.00[b]	25.00[b]
		H	25.00[b]	25.00[b]
		T	0.1000[a]	0.1584
	3, 4	B	10.00[a]	25.00[b]
		H	24.45	25.00[b]
		T	0.1000[a]	0.1000[a]
	5, 6	B	25.00[b]	25.00[b]
		H	25.00[b]	25.00[b]
		T	0.2577	0.1792
	7, 8	B	19.77	23.63
		H	25.00[b]	25.00[b]
		T	0.1000[a]	0.1000[a]
Final actuator masses, kg	1		0.7868	4.9571
	2 and 4		0.8526	8.2506
	3		0.8316	8.1153

[a]Lower bound values. [b]Upper bound values.

Table 5 Exponent c_2 vs final masses, $c_1 = 0.0047$ s^2/cm

c_2	Final mass, kg
0.700	161.29
0.750	162.44
0.800	162.63
0.850	164.36
0.875	164.57
0.900	165.65
0.925	165.89
0.950	166.68
0.975	169.32
1.000	170.17
1.025	171.85
1.050	173.95
1.075	176.12
1.100	179.47
1.125	186.35
1.150	194.58
1.175	204.41
1.200	215.26

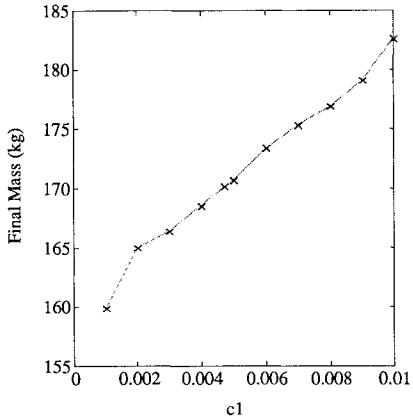

Fig. 2 Coefficient c_1 vs final masses.

force. Figure 3 shows that convergence is obtained in less than or equal to 17 analyses for all three cases.

Next, the value c_1 is fixed to be 0.0047 s^2/cm and the exponent c_2 values are varied between 0.7 and 1.2. Different c_2 values and their corresponding final optimal masses are given in Table 5 and Fig. 4. Final designs for $c_2 = 0.7$ and 1.2 are given in Table 6 and iteration histories for $c_2 = 0.7$, 1.0, and 1.2 are given in Fig. 5. Figure 4

Table 6 Final cross-sectional dimensions and actuator masses with different c_2 ($c_1 = 0.0047$ s^2/cm)

Design variables	Element/actuator number		$c_2 = 0.7$	$c_2 = 1.2$
Final cross-sectional dimensions, cm	1	B	25.00[b]	25.00[b]
		H	25.00[b]	25.00[b]
		T	0.1045	0.1000[a]
	2	B	25.00[b]	25.00[b]
		H	25.00[b]	25.00[b]
		T	0.1000[a]	0.1736
	3, 4	B	10.00[a]	25.00[b]
		H	21.13	25.00[b]
		T	0.1000[a]	0.1000[a]
	5, 6	B	25.00[b]	25.00[b]
		H	25.00[b]	25.00[b]
		T	0.2747	0.2297
	7, 8	B	18.06	24.12
		H	25.00[b]	25.00[b]
		T	0.1000[a]	0.1000[a]
Final actuator masses, kg	1		0.5147	9.0437
	2 and 4		0.5429	12.083
	3		0.9340	12.218

[a]Lower bound values. [b]Upper bound values.

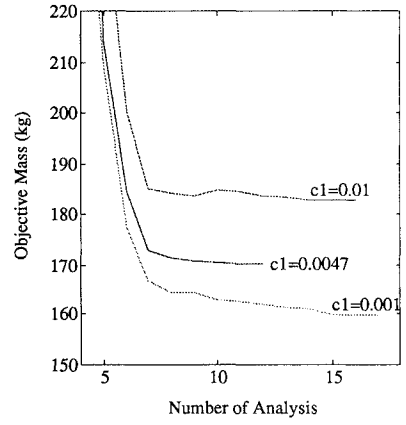

Fig. 3 Iteration histories with different c_1.

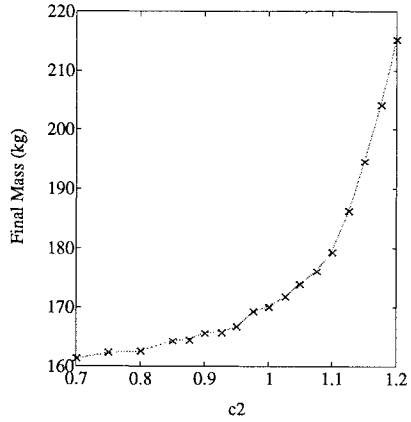

Fig. 4 Coefficient c_2 vs final masses.

shows that the final mass increases as the coefficient c_2 increases, especially when $c_2 \geq 1$. Also from Table 6, it is seen that the more strict actuator mass constraints require larger actuators as well as stiffer structural elements.

In the final run, the feedback gain matrix is modified in order to prevent uncontrolled higher modes from being destabilized. This run is the same as case 10 of Ref. 2 except that the feedback gain matrix

Table 7 Iteration history with modified feedback gain matrix

Analysis number	Design mass, kg
1	502.14
2	469.10
3	350.41
4	268.57
5	214.43
6	181.03
7	172.36
8	170.64
9	171.37
10	171.25
11	170.89
12	170.85
13	170.72
14	170.71
15	170.69

Table 8 Comparison of final complex eigenvalues, $\lambda_i = \sigma_i + j\omega_{di}$

Mode number	Case 10 of Ref. 2	Modified feedback gain matrix
1	$-2.73 \pm j1.61$	$-2.77 \pm j1.56$
2	$-1.86 \pm j4.97$	$-1.20 \pm j5.04$
3	$-0.683 \pm j23.7$	$-0.739 \pm j23.6$
4	$-0.519 \pm j50.1$	$-0.528 \pm j50.1$
5	$-0.866 \pm j64.7$	$-0.906 \pm j63.2$
6	$-1.08 \pm j103$	$-1.34 \pm j102$
7	$-0.933 \pm j184$	$-0.507 \pm j184$
8	$-0.623 \pm j241$	$-0.514 \pm j238$
9	$-2.50 \pm j320$	$-2.98 \pm j320$
10	$-2.25 \pm j324$	$-1.72 \pm j324$
11	$0.977 \pm j428$	$0.110 \times 10^{-3} \pm j427$
12	$0.076 \pm j619$	$-0.462 \times 10^{-3} \pm j618$
13	$0.183 \pm j637$	$-0.387 \times 10^{-3} \pm j626$
14	$0.203 \pm j681$	$0.395 \times 10^{-3} \pm j681$
15	$0.121 \pm j1015$	$0.438 \times 10^{-3} \pm j1000$
16	$0.121 \pm j1128$	$-0.670 \times 10^{-3} \pm j1121$
17	$0.504 \pm j1268$	$0.287 \times 10^{-3} \pm j1286$
18	$0.339 \pm j1375$	$0.971 \times 10^{-3} \pm j1378$

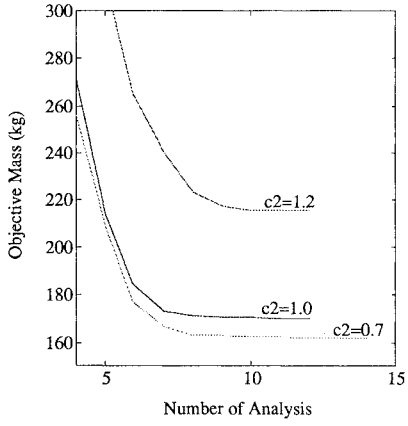

Fig. 5 Iteration histories with different c_2.

is modified according to Eqs. (22–24). Iteration history is given in Table 7 and the final closed-loop eigenvalues are compared with those of case 10 of Ref. 2 in Table 8. Most of the uncontrolled higher closed-loop eigenvalues (modes 11–18) of case 10 from Ref. 2 are slightly unstable, but with the modified feedback gain matrix real parts of the uncontrolled higher modes are very near zero so that these modes are marginally stable, i.e., by modifying the feedback gains, spillover effects are eliminated.

Conclusion

In Refs. 1 and 2, both structural and control system variables are treated as strictly independent design variables in the case of linear state feedback control via an adaptation of the design variable linking idea to the control system design variables. In the current study, actuator masses are also modeled as lumped nonstructural mass variables and treated as independent design variables in optimization by formulating actuator mass constraints in explicit form.

Numerical results generated by using the method presented here show the possibility of the design space integration including control system design variables, actuator masses as well as the conventional sizing variables.

The effect of choosing the coefficients c_1 and c_2 in actuator mass constraint formulation with the final optimal masses is shown graphically. It can be easily seen that the relation between c_1 and final masses is approximately linear and that as c_2 increases the optimal masses become larger exponentially. Also, a method to prevent instability of uncontrolled higher modes is introduced by modifying the feedback gain matrix without information about higher modes, which proved to be efficient for the example problem presented.

Acknowledgment

The sponsorship provided by the NASA Langley Research Center under NASA Grant 1490 is greatly acknowledged.

References

[1]Jin, I. M., and Schmit, L. A., "Control Design Variable Linking for Optimization of Structural/Control Systems," *AIAA Journal*, Vol. 30, No. 7, 1992, pp. 1892–1900.

[2]Jin, I. M., and Schmit, L. A., "Improved Control Design Variable Linking for Optimization of Structural/Control Systems," *AIAA Journal*, Vol. 31, No. 11, 1993, pp. 2111–2120.

[3]Lim, K. B., and Junkins, J. L., "Robustness Optimization of Structural and Controller Parameters," *Journal of Guidance, Control, and Dynamics*, Vol. 12, No. 1, 1989, pp. 89–96.

[4]Grandhi, R. V., "Structural and Control Optimization of Space Structures," *Computers and Structures*, Vol. 31, No. 2, 1989, pp. 139–150.

[5]Khot, N. S., "Minimum Weight and Optimal Control Design of Space Structures," *Computer Aided Optimal Design: Structural and Mechanical Systems*, NATO Advanced Study Inst. Series, Vol. F27, edited by M. Soares and C. A. Soares, Springer–Verlag, Berlin, 1987, pp. 389–403.

[6]Miller, D. F., and Shim, J., "Gradient-Based Combined Structural and Control Optimization," *Journal of Guidance, Control, and Dynamics*, Vol. 10, No. 3, 1987, pp. 291–298.

[7]Sepulveda, A. E., and Schmit, L. A., "Optimal Placement of Actuators and Sensors in Control Augmented Structural Optimization," *International Journal for Numerical Methods in Engineering*, Vol. 32, No. 6, 1991, pp. 1165–1187.

[8]Onoda, J., and Haftka, R. T., "An Approach to Structure/Control Simultaneous Optimization for Large Flexible Spacecraft," *AIAA Journal*, Vol. 25, No. 8, 1987, pp. 1133–1138.

[9]Sobieszczanski-Sobieski, J., Bloebaum, C. L., and Hajela, P., "Sensitivity of Control-Augmented Structure Obtained by a System Decomposition Method," *AIAA Journal*, Vol. 29, No. 2, 1991, pp. 264–270.

[10]Padula, S. L., James, B. B., Graves, P. C., and Woodward, S. E., "Multidisciplinary Optimization of Controlled Space Structures With Global Sensitivity Equations," NASA TP 3130, 1991.

[11]Grandhi, R. V., Haftka, R. T., and Watson, L. T., "Design-Oriented Identification of Critical Times in Transient Response," *AIAA Journal*, Vol. 24, No. 4, 1986, pp. 649–656.

[12]Balas, M. J., "Active Control of Flexible Systems," *Journal of Optimization Theory and Applications*, Vol. 25, No. 3, 1978, pp. 415–436.

[13]Schmit, L. A., and Farshi, B., "Some Approximation Concepts for Efficient Structural Synthesis," *AIAA Journal*, Vol. 12, No. 5, 1974, pp. 692–699.

[14]Schmit, L. A., and Miura, H., "Approximation Concepts for Efficient Structural Synthesis," NASA CR 2552, March 1976.

[15]Starnes, J. R., and Haftka, R. T., "Preliminary Design of Composite Wings for Buckling, Stress and Displacement Constraints," *Journal of Aircraft*, Vol. 16, No. 4, 1979, pp. 564–570.

[16]Vanderplaats, G. N., "CONMIN—A Fortran Program for Constrained Function Minimization," User's Manual, NASA TM X-62682, Aug. 1973.

[17]Lust, R. V., and Schmit, L. A., "Control Augmented Structural Synthesis," NASA CR 4132, April 1988.